Research Article | Vol. 25, No. 18 | 4 Sep 2017 | OPTICS EXPRESS 21826
Optics EXPRESS

Sub-shot-noise shadow sensing with quantum correlations

ERMES TONINELLI, MATTHEW P. EDGAR, PAUL-ANTOINE MOREAU, GRAHAM M. GIBSON, GILES D. HAMMOND, AND MILES J. PADGETT*

SUPA, School of Physics and Astronomy, University of Glasgow, Glasgow, G12 8QQ, UK
*Miles.Padgett@glasgow.ac.uk

Abstract: The quantised nature of the electromagnetic field sets the classical limit to the sensitivity of position measurements. However, techniques based on the properties of quantum states can be exploited to accurately measure the relative displacement of a physical object beyond this classical limit. In this work, we use a simple scheme based on the split-detection of quantum correlations to measure the position of a shadow at the single-photon light level, with a precision that exceeds the shot-noise limit. This result is obtained by analysing the correlated signals of bi-photon pairs, created in parametric downconversion and detected by an electron multiplying CCD (EMCCD) camera employed as a split-detector. By comparing the measured statistics of spatially anticorrelated and uncorrelated photons we were able to observe a significant noise reduction corresponding to an improvement in position sensitivity of up to 17% (0.8*dB*). Our straightforward approach to sub-shot-noise position measurement is compatible with conventional shadow-sensing techniques based on the split-detection of light-fields, and yields an improvement that scales favourably with the detector's quantum efficiency.

OCIS codes: (270.0270) Quantum optics; (120.3940) Metrology; (270.5290) Photon statistics; (270.2500) Fluctuations, relaxations, and noise; (030.5260) Photon counting; (280.4788) Optical sensing and sensors.

References and links

1. R. P. Middlemiss, A. Samarelli, D. J. Paul, J. Hough, S. Rowan, and G. D. Hammond, "Measurement of the Earth tides with a MEMS gravimeter," Nature **531**, 614–617 (2016).
2. V. Giovannetti, S. Lloyd, and L. Maccone, "Quantum-Enhanced Measurements: Beating the Standard Quantum Limit," Science **306**, 1330–1336 (2004).
3. R. E. Slusher, L. W. Hollberg, B. Yurke, J. C. Mertz, and J. F. Valley, "Observation of Squeezed States Generated by Four-Wave Mixing in an Optical Cavity," Phys. Rev. Lett. **55**, 2409–2412 (1985).
4. P. Grangier, R. E. Slusher, B. Yurke, and A. LaPorta, "Squeezed-light - Enhanced polarization interferometer," Phys. Rev. Lett. **59**, 2153–2156 (1987).
5. S. F. Pereira, M. Xiao, H. J. Kimble, and J. L. Hall, "Generation of squeezed light by intracavity frequency doubling," Phys. Rev. A **38**, 4931–4934 (1988).
6. K. W. Leong, N. C. Wong, and J. H. Shapiro, "Nonclassical intensity correlation from a type I phase-matched optical parametric oscillator," Opt. Lett. **15**, 1058–1060 (1990).
7. H. Vahlbruch, M. Mehmet, S. Chelkowski, B. Hage, A. Franzen, N. Lastzka, S. Goßler, K. Danzmann, and R. Schnabel, "Observation of Squeezed Light with 10-dB Quantum-Noise Reduction," Phys. Rev. Lett. **100**, 033602 (2008).
8. H. Vahlbruch, M. Mehmet, K. Danzmann, and R. Schnabel, "Detection of 15 dB Squeezed States of Light and their Application for the Absolute Calibration of Photoelectric Quantum Efficiency," Phys. Rev. Lett. **117**, 110801 (2016).
9. N. Treps, N. Grosse, W. P. Bowen, C. Fabre, H.-A. Bachor, and P. K. Lam, "A Quantum Laser Pointer," Science **301**, 940–943 (2003).
10. O. Schwartz and D. Oron, "Improved resolution in fluorescence microscopy using quantum correlations," Phys. Rev. A **85**, 033812 (2012).
11. O. Schwartz, J. M. Levitt, R. Tenne, S. Itzhakov, Z. Deutsch, and D. Oron, "Superresolution Microscopy with Quantum Emitters," Nano Lett. **13**, 5832–5836 (2013).
12. D. Gatto Monticone, K. Katamadze, P. Traina, E. Moreva, J. Forneris, I. Ruo-Berchera, P. Olivero, I. P. Degiovanni, G. Brida, and M. Genovese, "Beating the Abbe Diffraction Limit in Confocal Microscopy via Nonclassical Photon Statistics," Phys. Rev. Lett. **113**, 143602 (2014).

#304670 https://doi.org/10.1364/OE.25.021826
Journal © 2017 Received 17 Aug 2017; accepted 20 Aug 2017; published 29 Aug 2017

Optics EXPRESS

13. G. Brida, M. Genovese, and I. Ruo Berchera, "Experimental realization of sub-shot-noise quantum imaging," Nat. Photonics **4**, 227–230 (2010).
14. J.-L. Blanchet, F. Devaux, L. Furfaro, and E. Lantz, "Measurement of Sub-Shot-Noise Correlations of Spatial Fluctuations in the Photon-Counting Regime," Phys. Rev. Lett. **101**, 233604 (2008).
15. J.-L. Blanchet, F. Devaux, L. Furfaro, and E. Lantz, "Purely spatial coincidences of twin photons in parametric spontaneous down-conversion," Phys. Rev. A **81**, 043825 (2010).
16. O. Aytür and P. Kumar, "Pulsed twin beams of light," Phys. Rev. Lett. **65**, 1551–1554 (1990).
17. O. Jedrkiewicz, Y.-K. Jiang, E. Brambilla, A. Gatti, M. Bache, L. A. Lugiato, and P. Di Trapani, "Detection of Sub-Shot-Noise Spatial Correlation in High-Gain Parametric Down Conversion," Phys. Rev. Lett. **93**, 243601 (2004).
18. D. V. Strekalov, A. V. Sergienko, D. N. Klyshko, and Y. H. Shih, "Observation of Two-Photon "Ghost" Interference and Diffraction," Physical Review Letters **74**, 3600–3603 (1995).
19. T. B. Pittman, Y. H. Shih, D. V. Strekalov, and A. V. Sergienko, "Optical imaging by means of two-photon quantum entanglement," Physical Review A **52**, R3429–R3432 (1995).
20. K. Lyons, S. Pang, P. G. Kwiat, and A. N. Jordan, "Precision optical displacement measurements using biphotons," Phys. Rev. A **93**, 043841 (2016).
21. A. G. Basden, C. A. Haniff, and C. D. Mackay, "Photon counting strategies with low-light-level CCDs," Mon. Not. R. Astron. Soc. **345**, 985 (2003).
22. E. Lantz, J.-L. Blanchet, L. Furfaro, and F. Devaux, "Multi-imaging and Bayesian estimation for photon counting with EMCCDs," Mon. Not. R. Astron. Soc. **386**, 2262–2270 (2008).
23. M. Robbins and B. Hadwen, "The noise performance of electron multiplying charge-coupled devices," IEEE T. Electron Dev. **50**, 1227–1232 (2003).
24. M. Edgar, D. Tasca, F. Izdebski, R. Warburton, J. Leach, M. Agnew, G. Buller, R. Boyd, and M. Padgett, "Imaging high-dimensional spatial entanglement with a camera," Nat. Commun. **3**, 984 (2012).
25. E. Toninelli, "Sub-shot-noise shadow sensing with quantum correlations: EMCCD camera raw frames," Enlighten (2017) [retrieved 15/08/2017], http://dx.doi.org/10.5525/gla.researchdata.393 .
26. D. S. Tasca, M. P. Edgar, F. Izdebski, G. S. Buller, and M. J. Padgett, "Optimizing the use of detector arrays for measuring intensity correlations of photon pairs," Phys. Rev. A **88** 013816 (2013).
27. E. Lantz, P.-A. Moreau, and F. Devaux, "Optimizing the signal-to-noise ratio in the measurement of photon pairs with detector arrays," Physical Review A **90**, 063811 (2014).
28. A. Avella, I. Ruo-Berchera, I. P. Degiovanni, G. Brida, and M. Genovese, "Absolute calibration of an EMCCD camera by quantum correlation, linking photon counting to the analog regime," Opt. Lett. **41**, 1841–1844 (2016).

1. Introduction

The development of a simple and powerful technique that may allow an increase in the sensitivity of a conventional measurement device strongly motivates quantum physicists and engineers. One sensor type for which the quantised nature of light plays a role is the shadow-sensor: a sensor consisting of a light-source, a shadow-casting object, and a detector. Shadow-sensing can be employed to optically measure forces, by measuring small changes in the relative position of a shadow cast by a physical object, for example in the context of microelectromechanical system gravimeters [1]. The sensitivity of this technique relies on the measurement of the intensity of a light field, which ultimately depends on the ability to precisely count photons. However, this is not an easy task, because of the changes in the number of detectable photons caused by the quantised nature of the electromagnetic field (shot-noise) [2], and the presence of losses in the detection process. In fact, even in the case of a perfect detector able to generate a well-defined signal for each incoming photon, the sensitivity with which the intensity of an electromagnetic field can be measured will still be subject to this fundamental shot-noise limit. A noise suppression strategy used to beat the shot-noise limit in interferometry employs quantum squeezed states of light, allowing a reduction of the uncertainty in a monitored observable at the cost of the complementary observable. More than thirty years have been invested in the rigorous research of these squeezed quantum states [3–7], and a significant 15 dB noise suppression below the vacuum noise level has been harnessed using this approach [8]. This impressive achievement, however, comes at the cost of having to deal with an ultraprecise interferometric setup: a scheme that is technically very advanced, and therefore confined to the most sophisticated of laboratory settings.

In the last decade, a number of experiments have demonstrated the feasibility of noise reduction schemes using quantum correlations to achieve sub-shot-noise precision measure-

Optics EXPRESS

ments [9–12]. Brida et al. 2010 have experimentally demonstrated sub-shot-noise imaging using the spatially anticorrelated photon-pairs produced by spontaneous parametric downconversion (SPDC) in the specific case of a highly transmissive object and high photon-flux [13]. This use of intensity-correlated light fields produced by SPDC represents a technically simpler alternative to squeezing schemes based on homodyne detection, and a number of studies based on the photon-number spatial fluctuations of down-converted pairs have been investigated, using both type I [14, 15] and type II [16–20] non-linear crystals.

In this work we exploit the intensity correlations of parametric downconversion to experimentally demonstrate sub-shot-noise performance in the position measurement of a shadow produced by a fully opaque object and operating at the single-photon regime. We compare the performance of our noise reduction scheme to the classical case, by removing the photon-number correlation of the downconverted pairs and show a quantum-enabled enhancement in precision beyond the shot-noise limit.

2. Results

2.1. Experimental setup

The experimental setup used to demonstrate sub-shot noise sensitivity in the position measurement of a shadow is shown in Fig. 1.

A 160 mW, 355 nm laser (JDSU, xCyte CY-355-150) was attenuated to a few mW and used to pump a 10 mm × 10 mm × 3 mm β-barium borate (BBO) non-linear crystal, cut for type I degenerate downconversion. Two dichroic mirrors placed after the crystal (each 98% transmissive at 710 nm) were used to remove the UV pump. A stretched wire ($\approx$ 0.60 mm diameter) used to cast the shadow was placed at the far-field of the crystal, by using a 200 mm Fourier lens, and scanned across the field of view with a motorised linear stage (Newport, ESP300 controller, UE16CC motor). Due to the fact that the sensor of the EMCCD camera (Andor, ULTRA 888 DU-888U3-CS0-#BV; 13μm pixel size, 100% fill-factor) is recessed into the body of the camera by 17.4 mm, a 50 mm relay lens was used to re-image the plane of the scanning wire. A top-hat transmission profile interference filter (IF) (centred at 710 nm, with a 10 nm rectangular transmission band) was mounted on the camera to select the degenerate downconverted photon-pairs. In order to compare the noise performance of uncorrelated and anticorrelated light, a neutral density filter (ND2.0) was introduced either before or after the crystal, allowing to switch respectively between anticorrelated and uncorrelated light, while keeping a constant number of detected events. The chance of jointly detecting both photons of a photon-pair is thus reduced when the ND filter is placed after the BBO crystal by a factor of $10^{-2 \cdot OD}$, where OD is the optical density of the ND filter, causing the position anticorrelated light to become uncorrelated. Our system was optimised for the detection of anticorrelated photon-pairs, by minimising the spurious background light with a custom made light-tight enclosure and by optimising the camera's many acquisition settings, as shown in Appendix 4.1 and 4.2 respectively.

The EMCCD camera was operated as a single-photon resolved split-detector, by summing the events detected in the left and right halves of a square region of interest (ROI), and by using a single discriminating threshold above which an analogue count for a pixel would be considered as one detected photon [21, 22]. The threshold for binary detection of photons was chosen so as to maintain the quantum efficiency (QE) of detection, while minimising the excess noise introduced by the Gaussian readout noise of the camera, which dominates the low-count of the analogue-to-digital converter (ADC) counts histogram of EMCCD cameras. Under these conditions the chosen threshold was $T \geq 2\, SD_{readout} + \mu_{readout}$, where $SD_{readout}$ and $\mu_{readout}$ are the standard deviation and the mean of the electronic readout noise of the EMCCD camera, measured in ADC counts. By using an EMCCD camera we were both able to spatially characterise the single-photon quantum correlations of our source (as shown in Appendix 4.3), as well as demonstrate a noise reduction below the shot-noise limit with a split-detection scheme.

Optics EXPRESS

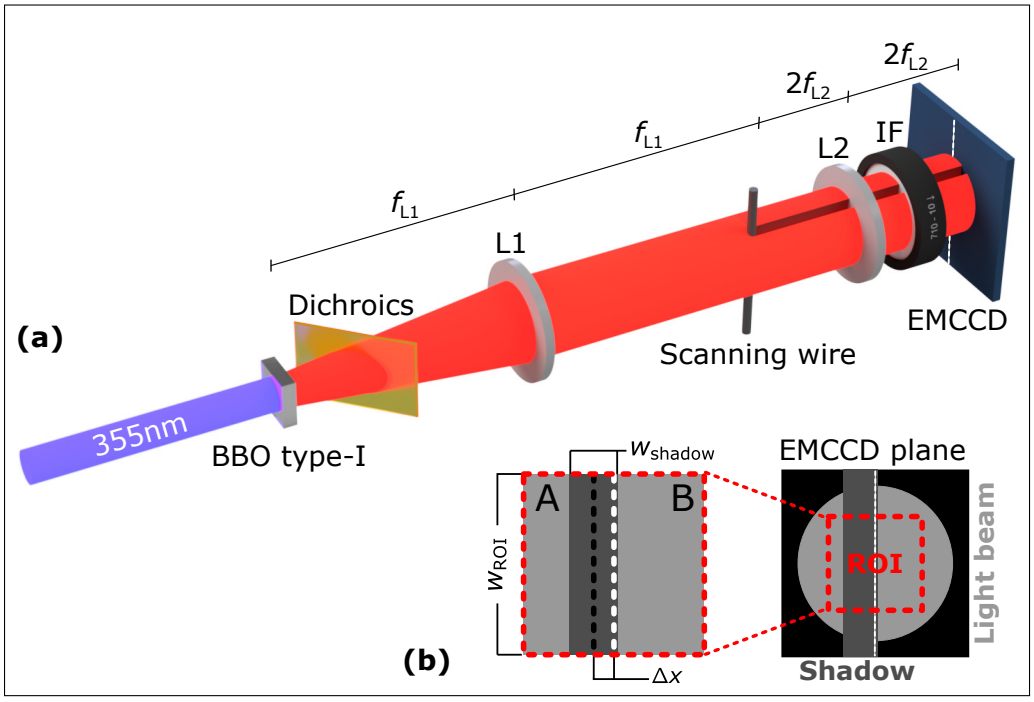

Fig. 1. Experimental setup used to measure noise reduction in the estimation of the position of a shadow. **(a)** The imaging system used to measure the position of the shadow cast by a scanning wire, consists of a 200 mm Fourier lens (L1) placed one focal length away from the crystal and the scanning wire; and a 50 mm relay lens (L2) placed two focal lengths away from the scanning wire and the plane of the EMCCD. A 10 nm band-pass interference filter (IF) centred at 710 nm was placed in front of the EMCCD. In order to compare the noise performance of uncorrelated and anticorrelated light, a neutral density filter (not shown in the figure) was introduced either before or after the crystal, allowing to switch respectively between position anticorrelated and uncorrelated light, while keeping a constant number of detected events. **(b)** The summed binary events, detected over the left and right halves of a square region of interest (A and B), were used to estimate the relative displacement of the shadow (Δx), for a certain width of the ROI (w_{ROI}) and width of the shadow (w_{shadow}).

Optics EXPRESS

Our scheme was hence designed to operate at a very low light level for the detection of single photons, such that within an exposure time at most one photon was detected by any pixel of the camera chip.

To avoid a signal imbalance between the two halves of the EMCCD camera, due to charge smearing effect [23, 24], the wire was oriented parallel to the readout direction and scanned through a square ROI (176 × 176 pixels or 2.29 mm × 2.29 mm, for the 13 μm pixel size of our camera) located at the centre of the downconverted beam, as shown at the top of Fig. 4. To optimise the detection of correlated photons the BBO crystal was slightly tilted with respect to the optical axis, increasing the transverse momentum component of the photon-pairs and obtaining a region at the centre of the downconverted beam of uniform intensity. In other words, we modify the downconverted beam from a Gaussian intensity profile (i.e. collinear phase matching) to a flat-top intensity profile (i.e. nearly collinear phase matching), minimising the number of two (or more) photon arrivals per pixel in the chosen central ROI of the EMCCD camera. The size of the ROI was matched to the so created nearly flat intensity area within the detected beam.

2.2. Analysis

In the present context of split-detection the square ROI in the detection plane was partitioned to give the summed number of photons A and B, such that $A + B = N$ and $\langle A\rangle + \langle B\rangle = \langle N\rangle$, where $\langle\ \rangle$ indicates temporal averaging over a number of frames.

Assuming a uniform illumination within the chosen ROI, the estimator for the relative displacement of the shadow from the centre Δx is then defined as:

$$\Delta x = \frac{A-B}{\langle A+B\rangle}\cdot l = \frac{A-B}{\langle N\rangle}\cdot l, \tag{1}$$

where $l = w_{ROI} - w_{shadow}2$, w_{ROI} is the width in pixels of the ROI, w_{shadow} is the width in pixels of the shadow cast by the wire, and N is the expected mean number of photons per frame within the ROI, as shown in Fig. 1(b). The use of the estimator shown in Eq. (1) is obviously restricted to the case in which the shadow is near the centre of the ROI, where the shadow does not fall entirely on either A or B, i.e. only valid for $\Delta x \leq w_{shadow}$. The position estimation depends upon the quantity $A - B$, and as the shadow of the wire is moved across the ROI, the noise statistics of the system can also be characterised from this same quantity.

The achievable amount of noise reduction is measured by comparing the performance of our system for both spatially anticorrelated and spatially uncorrelated photons, whilst keeping the total number of detected photons the same. Our detected photons are spatially anticorrelated when no extra optical losses are introduced to the downconverted pairs and the experiment is run at the maximum overall QE. Conversely, detected photons are spatially uncorrelated when the downconverted pairs are strongly attenuated by introducing the neutral density filter between the downconversion crystal and the camera, while increasing the pump power so as to maintain the overall flux. The two configurations described above allow us to compare the noise of our system for high and low values of QE and make an estimation of the corresponding quantum advantage in position estimation. For a coherent state, attributed to be the best classical state for noise performance [16], the anticipated error in estimating a photon-number difference is given by:

$$\left\langle \Delta\,(A-B)^2 \right\rangle = \langle A\rangle + \langle B\rangle\,. \tag{2}$$

Equation (2) is characteristic of Poissonian statistics and defines the so called shot-noise limit (SNL), for which the variance of the residual difference of the detected events over the two halves of a split detector (left-hand side of Eq. (2) is equal to mean number of the total

Optics EXPRESS

number of detected events (right-hand side of Eq. (2)). Accordingly, in the present context sub-shot noise position sensitivity is achieved if:

$$\sigma \equiv \frac{Var(A-B)}{\langle A+B \rangle} < 1, \tag{3}$$

where σ (not to be confused with standard deviation, which in this work is indicated using the SD abbreviation) is the degree of correlation or the quantum noise reduction factor [13], defined as the variance of the photon-number difference normalised to the mean number of detected photons, and $Var(\ )$ indicates the variance computed over a number of frames. In the case of additional attenuation of the downconverted photon-pairs the detected events at the EMCCD are mainly uncorrelated photons, statistically similar to a classical case.

The total QE of the detection line of our system (including optical losses, parasitic light, detector's losses, and the losses introduced by applying a photon discriminating threshold to the acquired frames) was conservatively estimated to be 26%. This value was calculated using Eq. (4) [13] and our experimentally determined degree of correlation for the unattenuated and unobstructed beam $\sigma_{un.}$.

$$QE_{total} = 1 - \sigma_{un.} = 1 - 0.73 = 26\% \tag{4}$$

Hence the amount of achievable noise reduction of our scheme depends on QE_{total}, which limits the ability to detect quantum correlations. Importantly this scheme would operate even in the presence of higher losses, yielding an advantage with respect to an equivalent spatially uncorrelated source. In fact, even in the presence of high optical losses, there will always be a non-zero probability of jointly detecting both signal and idler photons of a number of photon-pairs, hence achieving noise suppression.

2.3. Experimental results

Firstly, we demonstrated the ability of our system to attain a fractional degree of correlation (i.e. $\sigma \leq 1$) using the unobstructed and unattenuated downconverted beam. The results are shown in Fig. 2.

It can be seen that anticorrelated light shows a noise below the shot-noise limit, whereas uncorrelated light exhibits noise above the shot-noise limit. A noise level above the shot-noise limit is indicative of excess noise, as discussed in Appendix 4.4. In our care this includes noise from the laser and noise from the EMCCD camera. It may be useful to note that our laser is an air-cooled industrial laser with a pulse repetition of 100 $Mhz \pm 10\ MHz$. Concerning our detector, we noticed less than ideal noise performance for high levels of EM gain. However, in order to minimise the number of missed detections of photons, it was necessary to employ the highest available EM gain. Moreover, due to the chosen light level of 0.15 photons per pixel per frame, the noise of the detector (i.e. uncorrelated dark events) was not found to play a significant role in the statistics of the detected events, as the dark-count rate for our optimised detector was only 0.0045 events per pixel per frame. The light level was chosen so as to avoid unwanted saturation effects of the detector and hence ensuring maximum noise suppression when compared to the same level of uncorrelated light.

Secondly, the wire was scanned across the selected ROI, allowing the characterisation of the noise performance of the system. The position estimator for a full scan of the wire is shown in Fig. 3. The restricted position range over which the position estimator described in Eq. 1 can be used is highlighted in Fig. 3 by the two vertical dotted lines.

The noise performance of our system is shown in Fig. 4 as a function of the wire's position. It can be observed that in the case of anticorrelated light and over the full range of positions the noise level is better than the shot-noise limit, whereas in the case of uncorrelated light the

Optics EXPRESS

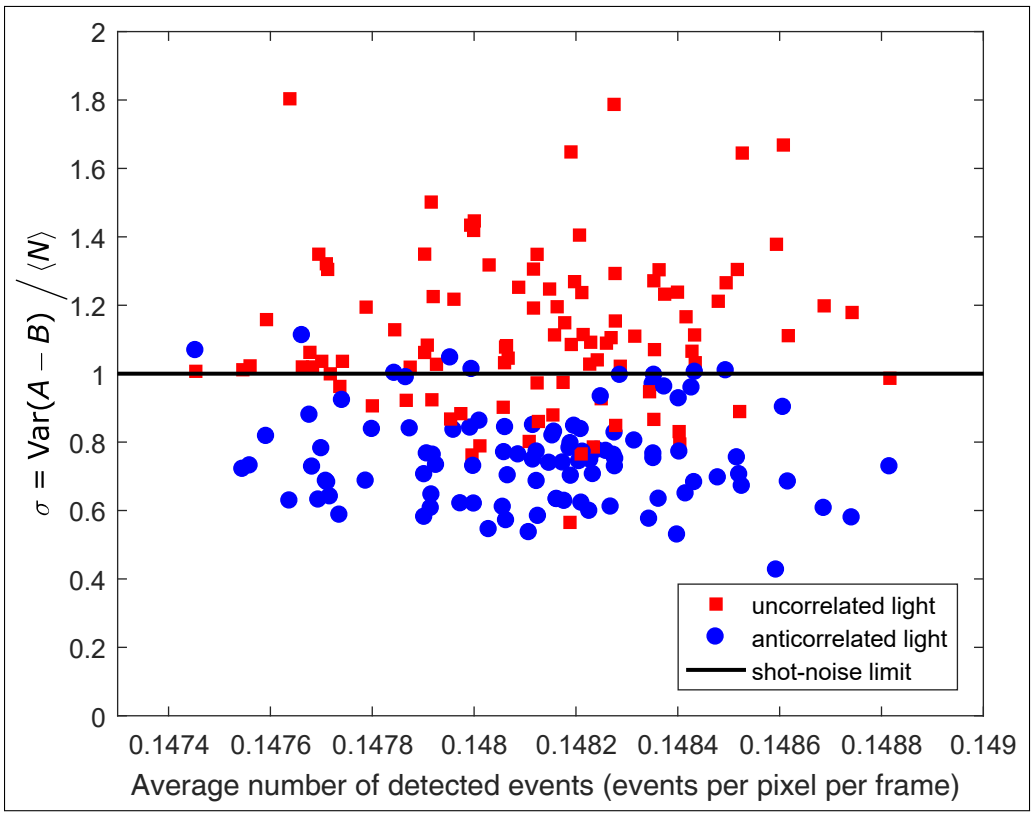

Fig. 2. Characterisation of the degree of correlation for the anticorrelated and uncorrelated light sources. The anticorrelated data shows a clear noise reduction with respect to both the uncorrelated data and the shot-noise limit. Each point of the variance of $(A-B)$ normalised to the shot-noise was calculated over 50 frames. The x-axis shows the average number of detected events (i.e. photons + dark-counts).

noise level is worse than the shot-noise limit. A noise reduction beyond the shot-noise limit is therefore demonstrated using quantum correlations, for every position of the shadow.

Lastly, the frame to frame fluctuations for the three central positions of the shadow are shown in Fig. 3, and correspond to the yellow highlighted range in Fig. 5.

The photon-number fluctuations of uncorrelated light are visibly greater than those associated to anticorrelated light. This means that the sensitivity of the position estimation of the shadow, based on the values of A and B, is better for anticorrelated light. The enhancement in position sensitivity $\mathcal{E}$, which is proportional to $\langle A-B\rangle$, can be calculated as follows:

$$\mathcal{E} = 1 - \frac{SD_{\Delta x_{AC}}}{SD_{\Delta x_{UC}}} = 1 - \frac{SD_{(A-B)_{AC}}}{SD_{(A-B)_{UC}}} = 1 - \frac{\sqrt{\sigma_{AC}}}{\sqrt{\sigma_{UC}}}, \tag{5}$$

where $SD_{\Delta x}$ is the uncertainty associated to the estimated position of the shadow, $SD_{(A-B)}$ is the square root of the normalised variance of $A-B$, $\sqrt{\sigma}$, and the subscripts AC and UC indicate anticorrelated and uncorrelated data respectively. Using Eq. (5) and the values from Fig. 4, the maximum enhancement in position sensitivity for the central position of the wire was calculated as shown in Eq. (6):

Optics EXPRESS

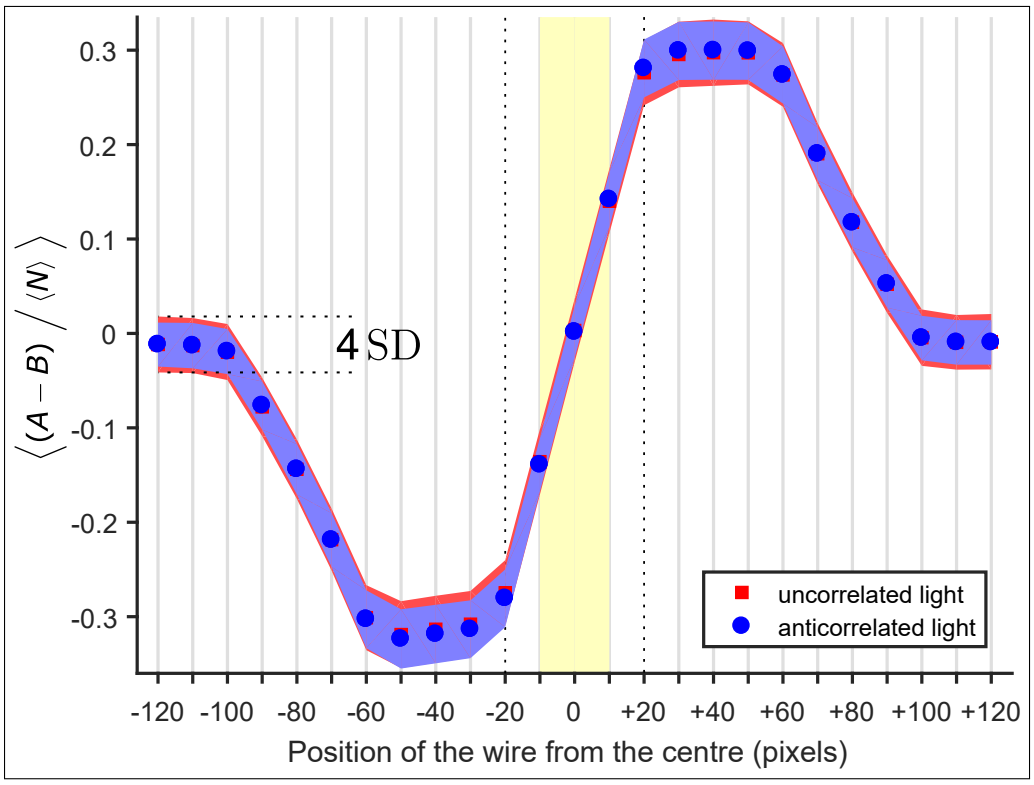

Fig. 3. Characterisation of the position estimator. The mean of the normalised residual difference is plotted as a function of the position of the scanning wire. The values of A and B allow to estimate the position of the wire within the position range delimited by the dotted lines, as described by Eq. (1). Four times the standard deviation (SD) was chosen to highlight the precision of the measurements. The yellow-shaded interval is used in Fig. 5 to show the frame to frame fluctuations of the position estimator.

$$\mathcal{E}_0 = 1 - \frac{\sqrt{0.79}}{\sqrt{1.14}} = 16.8\%(\pm 2\%) \quad (i.e.\ 0.80\ dB) \tag{6}$$

Alternatively, by assuming a potential $\sigma_{UC} = 1$, the quantum enhancement in position sensitivity is still better than the shot-noise level of the equivalent shot-noise limited scheme and is calculated as shown in Eq. (7):

$$\mathcal{E}_{SNL} = 1 - \frac{\sqrt{0.79}}{\sqrt{1.00}} = 11.1\%(\pm 1\%) \quad (i.e.\ 0.51\ dB) \tag{7}$$

The errors for $\mathcal{E}_0$ and $\mathcal{E}_{SNL}$ were computed at one SD of confidence. It should be noted that an enhancement in the estimation of the position of the wire is achieved for every position of the scanning wire.

Optics EXPRESS

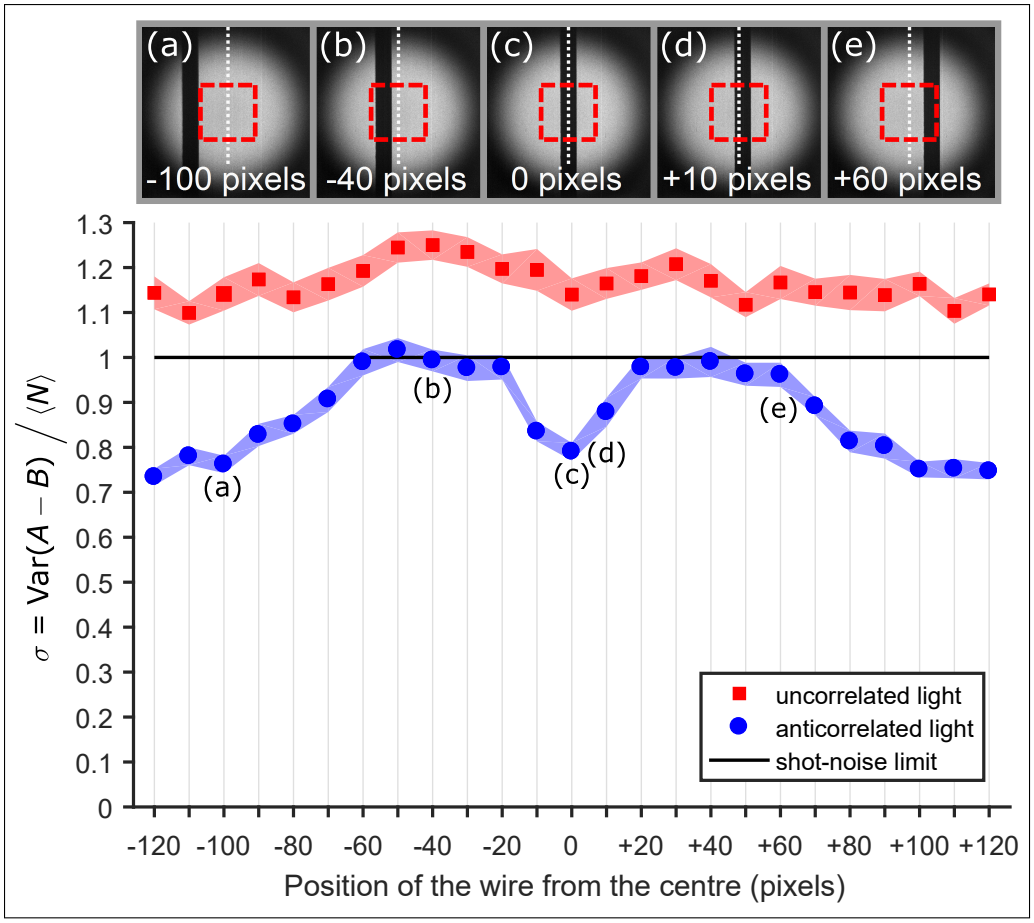

Fig. 4. Noise performance for anticorrelated and uncorrelated light as a function of wire position. The wire is scanned at increments of 10 pixels across the field of view for both position anticorrelated and uncorrelated light, as shown in the upper part of the figure. Each point in the graph corresponds to the estimation of the normalised variance of $A - B$ (i.e. the degree of correlation σ) each averaged over 2500 frames. The shaded areas indicate the confidence intervals at two SDs. The anticorrelated data shows noise suppression below both the uncorrelated counterpart and the shot-noise limit. The top-row shows five key positions of the scanning wire as detected by the EMCCD camera, and the red-dashed squares highlight the chosen ROI. A discussion of these positions of the scanning wire in terms of achievable noise suppression is provided in Appendix 4.5.

Optics EXPRESS

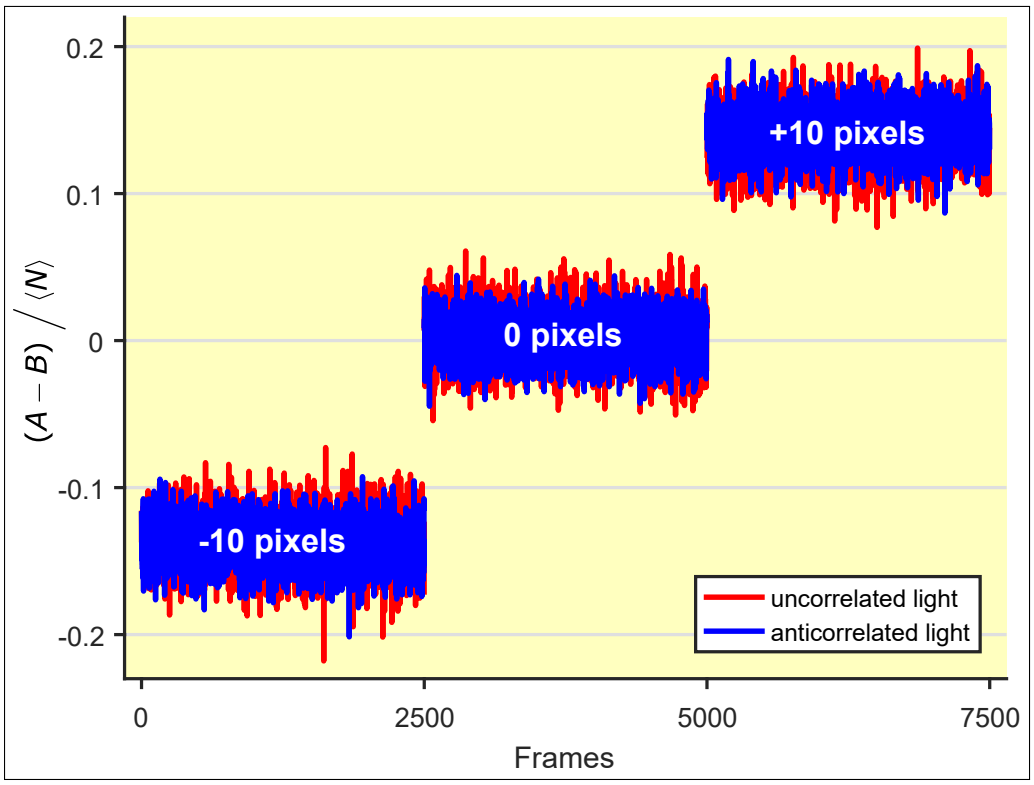

Fig. 5. Fluctuations of the position estimator from frame to frame. The frame to frame normalised residual difference between A and B is plotted for the central position range highlighted in Fig. 3. Anticorrelated data shows a precision improvement in the position estimation of the wire compared to uncorrelated data.

3. Conclusion

We have demonstrated the ability to exploit quantum correlations to improve the precision in the estimation of the position of a shadow cast by a fully opaque object at very low light levels, i.e. at less than one photon per pixel per frame. We acknowledge that in many optical systems it is possible to improve the noise statistics by simply increasing the light flux, however this may not always be possible. The performance of various systems operating at high flux can be compromised by a host of additional unwanted effects, such as increased radiation pressure, increased thermal loading, greater power consumption or creating biological damage, for all of which the ability to operate at low flux could have importance. Furthermore, noise reduction schemes based on quantum correlations are not only limited to low-light settings, but could provide an additional advantage in the context of bright-light sensing schemes.

In conclusion, by comparing the noise performance of position anticorrelated and uncorrelated light, we have experimentally demonstrated a 17% ($0.8dB$) enhancement in the position sensitivity of a shadow using quantum correlations from an SPDC source. The quantum advantage of our noise-suppression scheme was found to scale favourably with the effective total quantum efficiency of the detection line. This is because the performance of our sub-shot-noise shadow sensor depends on the ability to jointly detect the signal and idler photons of an as large number as possible of downconverted pairs. Our approach to quantum-enhanced position measurement effectively addresses the EMCCD as a split-detector, paving the way to real-

world applications of quantum-enhanced position measurement, for which less expensive detectors, such as high-responsivity/low-noise split-photodiodes, are sought to enable wide-spread use. Moreover, our noise reduction technique is compatible with existing shadow-sensor based measuring devices [1]: for example, a quantum correlated source could be installed onto a conventional shadow sensor, yielding an immediate precision advantage, only limited by the QE of the employed split-detector. To the best of our knowledge this work represents the first experimental demonstration of quantum noise reduction in the position measurement of a shadow using spatially anticorrelated photon-number correlations at the single-photon regime. All raw frames data that support the findings of this study have been deposited in Enlighten [25].

4. Appendix

4.1. *Light-tight enclosure*

In order to reduce parasitic light and unwanted fluorescence from the UV pump, care was taken in the design of a light-tight enclosure, which is shown in Fig. 6. The closely fitting lids of the light-tight enclosure were constructed so as to eliminate a direct line-of-sight, with multiple 90-degree light-stops, preventing stray light from entering the enclosure. Light-absorbent foam seals were applied along all of the joints, including between panels, lids, supporting metal frame, and the underlying optical bench. Additionally, light-tight rubber bellows were used to link the optical components used in the EMCCD side of the enclosure. In order to ensure proper cooling of the laser and EMCCD camera within the sealed enclosure, we extracted the heat by means of water cooling (EMCCD) and air-ducting (laser).

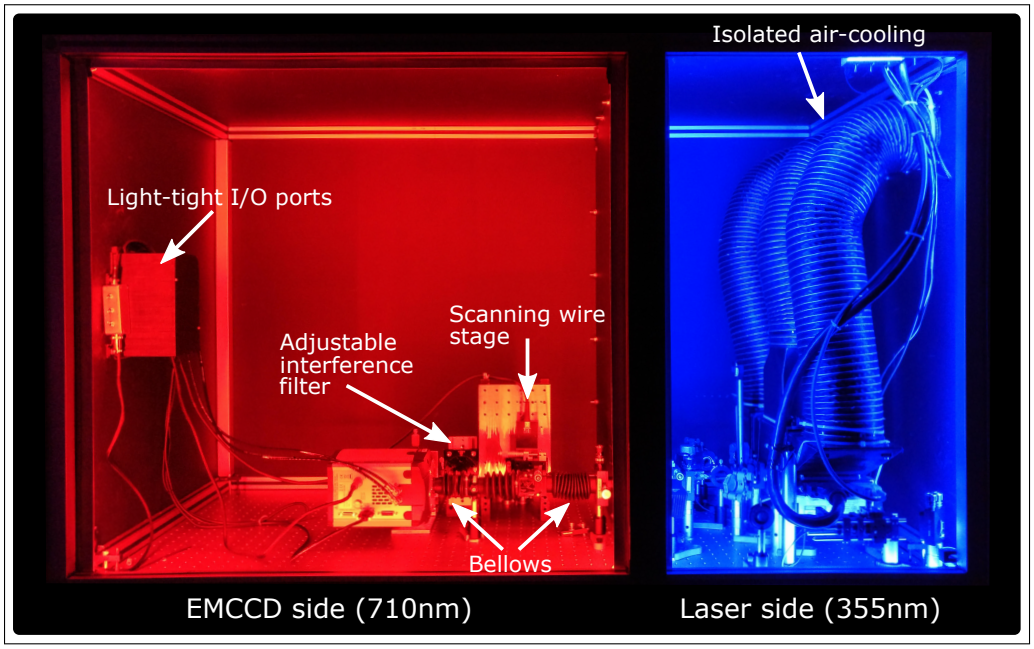

Fig. 6. Light-tight enclosure. The experiment enclosure is divided into two light-tight compartments by a blackened metal sheet partition: UV pump laser side (blue) and downconverted-light side with the EMCCD detector (red). The enclosure is constructed from metal frame clad with blackened wooden panels. Care was taken to eliminate stray light by employing custom light-tight I/O ports and designing an isolated air-cooling system for the laser.

Optics EXPRESS

4.2. EMCCD camera acquisition settings

The camera temperature was stabilized at −90 °C using both the built-in fan (set to maximum) and liquid cooling (15 °C water coolant); the acquisition mode was set to frame transfer enabled; the frame transfer mode was set to kinetics; the exposure time was set to 56.795 ms, which is the shortest exposure achievable for a 512 × 512 pixels frame size, using the frame transfer acquisition mode; the vertical speed was set to 1.13333 μs; the voltage clock-amplitude was set to 0 V; the horizontal speed was set to 10 MHz; the baseline-offset was set to 0 electrons; the baseline-clamp was enabled; the EM gain was set to its maximum value of 1000; and the pre-amplifier gain was set to 1, so as to generate one ADC count for every 16.1 electrons.

4.3. Strength of spatial correlations in the momentum plane of the crystal

A noise reduction scheme based on anticorrelated intensity beams relies on the ability to detect a large number of anticorrelated events. The objective is to maximise the number of joint detections of photon-pairs, while minimising the number of detected single events. Pair events are the downconverted photon-pairs. Single events can be any of the following: 1) detector dark events, such as thermalised photoelectrons or clock-induced-charges; 2) partially detected photon-pairs, due to optical or detector's losses; 3) uncorrelated photon events, due to spurious background illumination, such as fluorescence, ambient light, or longer wavelength light present in the UV pump laser. The optimisation of EMCCD cameras in terms of acquisition parameters and the optimal choice of a single photon-discriminating threshold have been extensively investigated in the literature [22, 23, 26, 27].

In order to ensure an optimal level of degree of correlation for our shadow sensor, we proceeded by optimising our system using the strength of detected anticorrelated events as a metric. Both optical losses and spurious background illumination can be mitigated by careful adjustment and alignment of the optical channel. The optimisation included fine adjusting of the position of the Fourier and relay lenses with respect to the detector, as well as tilting by few degrees the interference filter placed before the detector, to maximise the joint-detection of downconverted pairs at degeneracy, with respect to the filter's transmission window. We tested several interference filters and found that, due to small variations in the thickness of the filter's layers, the central wavelength differed from the nominal value at times by a few nanometres. Moreover, it may be useful to note that the effective QE of detector arrays operated with a photon-counting discriminating threshold may be considerably lower than that indicated by manufacturers [28].

The correlation peaks of detected photon-pairs in the momentum plane of the crystal are shown in Fig. 7 for our optimised system. We observed a strong single-frame correlation ($SNR = 4.34$) confirming the ability of our system to jointly detect a large number of anticorrelated photon-pairs.

4.4. Excess noise

We characterised the photon counting statistics of our system by measuring the variance of detected events from frame to frame, and confirmed the presence of noise in our system, attributed to the power stability of our laser ±10% and the noise performance of our camera. More specifically, considering the temporal statistics of our system (i.e. over a significant number of captured frames) we found the variance of the total number of detected events to be greater than the average number of detected events, for both correlated and uncorrelated light, albeit slightly greater in the case of correlated light, for which shot-noise is also correlated. In the case of dark-frames (with the laser powered-off and the camera's shutter closed) we measured a statistic similar to uncorrelated light, and attributed these fluctuations to the non-linearity of the electron multiplying gain for high levels of gain. In spite of our laser and camera not operating at the shot-noise limit, we were still able to differentially measure sub-shot-noise levels of quantum noise reduction, thanks to sufficient detection of correlated photon pairs.

Optics EXPRESS

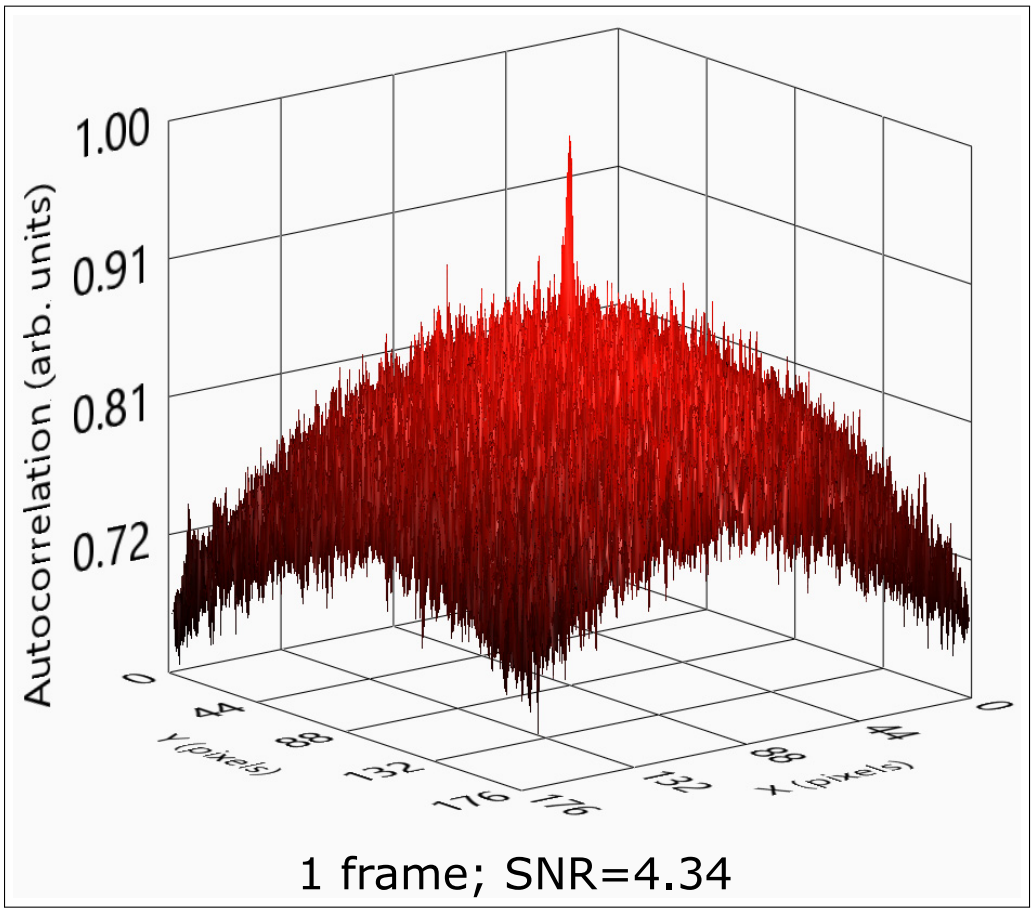

Fig. 7. Experimental evidence of strong anticorrelation of photon-pairs as detected in the far-field of the downconversion crystal. The correlation of a single frame detected by our EMCCD camera is shown. The whole optical channel was optimised to minimise losses, resulting in a strong single-frame correlation peak ($SNR = 4.34$) at 0.15 events per pixel per frame. The SNR is computed considering the height of the correlation peak with respect to the noise of the Gaussian pedestal.

Optics EXPRESS

4.5. Noise statistics for anticorrelated light at five key positions of the scanning wire

A detailed description of the five key positions shown in Fig. 8 in terms of noise suppression are described as follows: when the wire is completely outside of the ROI (Fig. 8 (a)) the noise suppression is greatest, as none of the downconverted pairs is intercepted by the wire; as the wire enters the ROI (Fig. 8 (b) an increasing number of correlated pairs is intercepted, causing the correlated events on the other half of the detector to build up an imbalance in the noise statistic; when the wire is at the centre (Fig. 8 (c)) an equal number of photons is intercepted over the two halves of the detector, resulting in a balanced noise statistic. Sub-pixel offset in the centring of the wire and uncorrelated events introduced by photons diffracted at the edges of the wire can cause the noise suppression at this position to be slightly worse than for the case of the wire being completely outside of the ROI; for positions of the wire near the centre of the ROI (Fig. 8 (d)) the noise suppression remains significant, as a sufficient number of correlated events can be detected, in spite of photon-pairs being intercepted by the wire on either side of the ROI; the lowest noise reduction is found when the wire intercepts the greatest number of downconverted pairs: i.e. when the whole width of the wire is on either side of the ROI (Fig. 8 (e)), intercepting the greatest number of photon-pairs and consequently generating the greatest number of single uncorrelated events.

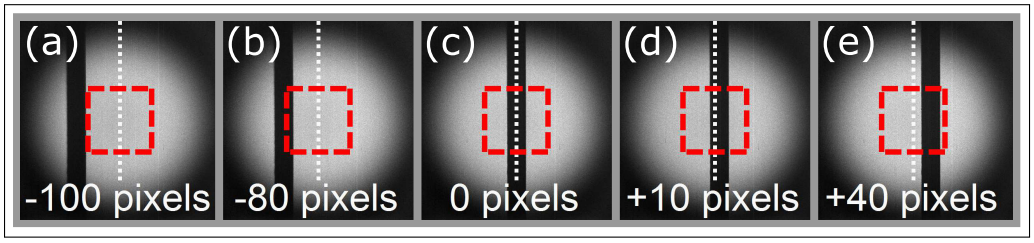

Fig. 8. Five key positions of the scanning wire as detected by the EMCCD camera. The amount of noise suppression depends on the number of jointly detected photon-pairs, which in turn depends on the position of the scanning wire. The red-dashed squares highlight the chosen region of interest. The numbers at the bottom indicate the positions of the scanning wire from the central white-dotted line.

Disclosures

The authors declare that there are no conflicts of interest related to this article.

Funding

Engineering and Physical Sciences Research Council (EP/L016753/1, EP/M01326X/1); European Union's Horizon 2020 Research and Innovation Programme (706410); European Research Council (TWISTS, 340507).

Acknowledgements

E.T. acknowledges the support from the EPSRC Centre for Doctoral Training in *Intelligent Sensing and Measurement* (Grant No. EP/L016753/1). M.P.E. acknowledges support from EPSRC QuantIC (EP/M01326X/1) and ERC TWISTS (Grant No. 192382). P.A.M. acknowledges the support from the European Union's Horizon 2020 research and innovation programme under the Marie Sklodowska-Curie (Grant No. 706410). All Authors acknowledge the funding from the European Research Council (TWISTS, Grant No. 340507).

Optics EXPRESS

We would like to thank Dr Matthias Sonnleitner and Prof Steve Barnett for helpful discussions about Poissonian noise statistics. We would also like to thank Dr Richard P. Middlemiss for useful discussions about the *WeeG* gravimeter device.